PHYSICAL REVIEW D VOLUME 47, NUMBER 8 15 APRIL 1993

Apparent horizons of an N-black-hole system in a space-time with a cosmological constant

Ken-ichi Nakao
Department of Physics, Kyoto University, Kyoto 606, Japan

Kazuhiro Yamamoto
Uji Research Center, Yukawa Institute for Theoretical Physics, Kyoto University, Uji 611, Japan

Kei-ichi Maeda
Department of Physics, Waseda University, Tokyo 169-50, Japan
(Received 23 October 1992)

We present the analytic solution of N Einstein-Rosen bridges ("N black holes") in the space-time with a cosmological constant Λ and analyze it for one- and two-bridge systems. We discuss the three kinds of apparent horizons: i.e., the black-hole, white-hole, and cosmological apparent horizons. In the case of two Einstein-Rosen bridges, when the "total mass" is larger than a critical value, the black-hole apparent horizon surrounding two Einstein-Rosen bridges is not formed even if the distance is very short. Furthermore, in this case, the cosmological apparent horizon enclosing both bridges does not appear. Hence, it seems that when the "total mass" is very large, the Einstein-Rosen bridges cannot collapse into one black hole unless the "gravitational mass" is released in some way.

PACS number(s): 98.80.Hw, 04.20.Jb, 04.30.+x

I. INTRODUCTION

Our Universe observed today is homogeneous and isotropic. The standard big bang scenario is based on this observational fact and can explain important observational facts, i.e., Hubble's expansion law, 2.7-K cosmic microwave background radiation, and the abundance of light elements. However, since homogeneity is the basic principle in the big bang scenario, we cannot get a natural answer within the framework of this scenario for the question of why our Universe is so homogeneous at present. The inflationary-universe scenario is one of the most favorable models to resolve the above question, the so-called homogeneity problem [1]. In this scenario, the vacuum energy due to the phase transition by an inflaton scalar field dominates at very early stages of the Universe. Since the vacuum energy of the inflaton field behaves like the cosmological constant, the Universe undergoes de Sitter-like rapid cosmic expansion. After a phase transition, the vacuum energy is converted into radiation and the standard big bang model is recovered. Initial inhomogeneities are stretched and go outside the horizon by rapid cosmic expansion, resulting in the present homogeneity of the Universe.

However, even through there is a positive cosmological constant, it is not obvious whether or not the de Sitter-like rapid cosmic expansion is always realized. Since the inhomogeneities have "energy" and generate the gravitational field by themselves, those may collapse into a black hole or a naked singularity. In connection with this problem, the "cosmic no hair conjecture" has been proposed, which states that "all" space-times approach the de Sitter space-time asymptotically if a positive cosmological constant exists [2]. If this conjecture is true or almost true, we can understand why the present Universe is so homogeneous.

In the realistic inflationary scenario, the cosmological constant is given by the vacuum energy of the inflaton field and hence the inhomogeneity of the cosmological "constant" itself is important for the onset of inflation. So several authors have investigated the inhomogeneities of the inflaton field both in analytic and numerical approaches [3–5]. However, inhomogeneities other than the cosmological constant are important too because, when we discuss the onset of inflation, such inhomogeneities may also not be so small before the de Sitter-like rapid expansion. As for the inhomogeneity by a dust fluid in space-time with a cosmological constant, we have an analytic approach which shows that some inhomogeneities collapse into a black-hole space-time [6,7]. The gravitational waves, which are the inhomogeneities of the space-time itself, can also form a black-hole space-time [8].

In this paper, in order to investigate the behavior of inhomogeneity in the space-times with a cosmological constant Λ and get some physical insight about a many-black-hole system in de Sitter background, we present initial data for Einstein-Rosen bridges in space-time with Λ. By the appropriate choice of the extrinsic curvature, the Hamiltonian constraint for the vacuum space-time with Λ turns out to be that of the time symmetric initial value problem without Λ and the momentum constraint becomes trivial. Hence, even through there is Λ, we can easily obtain an N-Einstein-Rosen-bridge solution for the constraint equations as the time symmetric initial value problem without Λ.

Since the Einstein-Rosen bridges have homotopically nontrivial structures, those topological structures do not disappear in the course of their time evolution within the framework of the classical Einstein theory. However, we

may obtain some physical insight for how inhomogeneities can grow up as we will show in this paper. We investigate the existence of the apparent horizons in the case of one- and two-Einstein-Rosen-bridge solutions. From its analysis, we may see a cosmic expansion effect on the inhomogeneities due to Einstein-Rosen bridges. The one-Einstein-Rosen-bridge solution corresponds to a three-dimensional spacelike hypersurface of the Schwarzschild–de Sitter space-time. This example shows us that the Einstein-Rosen bridge with a very large "gravitational mass" does not collapse into a singularity but rather expands and approaches the de Sitter space-time locally under the condition of a uniformly expanding background universe. For the two-Einstein-Rosen-bridge case, we find that a black hole apparent horizon surrounding two Einstein-Rosen bridges with a sufficiently large "total mass" does not appear for any distance of two bridges. Furthermore, the cosmological apparent horizon surrounding two Einstein-Rosen bridges also does not exist in such a circumstance. This feature is essentially the same as the one-Einstein-Rosen-bridge case and, hence, it seems that when the total mass is larger than a critical value, the two Einstein-Rosen bridges do not collapse into one black hole.

This paper is organized as follows. In Sec. II, we construct the initial data for N Einstein-Rosen bridges embedded in a uniformly expanding background universe with Λ. In Sec. III, we analyze the existence of the apparent horizons for one and two Einstein-Rosen bridges. Although the one-Einstein-Rosen-bridge solution is just a three-dimensional spacelike hypersurface of the Schwarzschild–de Sitter space-time, it gives us important insight for apparent horizons in an N-black-hole system. We, hence, show the basic feature of the Schwarzschild–de Sitter space-time in Appendix A. The method to obtain the apparent horizons for the two-Einstein-Rosen-bridge solution is presented in Appendix B. Some discussion and remarks are given in Sec. IV. In this paper, we adopt the units of $c=G=1$. Our conventions for the Riemann tensor and Ricci tensor are

$$D_{[i}D_{j]}v_k=\tfrac{1}{2}R^{l}_{ijk}v_l\ ,\qquad R_{ij}=R^{l}_{ilj}\ , \tag{1.1}$$

where D_i is the covariant derivative.

II. INITIAL DATA FOR AN N EINSTEIN-ROSEN BRIDGE IN A UNIFORMLY EXPANDING UNIVERSE

Initial data for vacuum space-times with a cosmological constant Λ must satisfy the Hamiltonian and momentum constraints: i.e.,

$$^{3}R-K^{j}_{i}K^{i}_{j}+K^{2}=6H^{2}\ , \tag{2.1}$$

$$D_j(K^{j}_{i}-\delta^{j}_{i}K)=0\ , \tag{2.2}$$

with

$$H\equiv\left[\frac{\Lambda}{3}\right]^{1/2}\ , \tag{2.3}$$

where $^{(3)}R$ is the Ricci scalar of the three-dimensional spacelike hypersurface. K^{j}_{i} is the extrinsic curvature of the three-space and K is its trace part. D_j is the covariant derivative with respect to the intrinsic metric of the three-space.

Here we consider the case with the extrinsic curvature which has only a trace part: i.e.,

$$K^{j}_{i}=-H\delta^{j}_{i}\ . \tag{2.4}$$

By virtue of the above condition, the Hamiltonian constraint reduces to the same as that of the time symmetric initial value for the vacuum space-time without Λ: i.e.,

$$^{(3)}R=0\ , \tag{2.5}$$

and the momentum constraint is satisfied trivially.

In order to solve Eq. (2.5), we assume the conformally flat metric

$$dl^2=\psi^4[dr^2+r^2(d\theta^2+\sin^2\theta\, d\varphi^2)]\ , \tag{2.6}$$

where dl^2 is the three-metric of the initial surface. With this metric, the Hamiltonian constraint (2.5) becomes the Laplace equation: i.e.,

$$\Delta\psi=0\ , \tag{2.7}$$

where Δ is the flat Laplacian.

Here, it should be noted that, for an isotropic and homogeneous space-time in which the scale factor $a=\psi^2$ is spatially constant, the condition (2.4) turns out to be the Friedmann equation in terms of cosmic time t, i.e., $a^{-2}(da/dt)^2=H^2$, resulting in the de Sitter solution ($a=e^{Ht}$). Thus, the condition (2.4) is regarded as the assumption of a uniformly expanding background universe.

As for the time symmetric initial value problem without Λ, we know how to obtain the N-Einstein-Rosen-bridge solution, which is just to set ψ as [9]

$$\psi=1+\sum_{i=1}^{N}\frac{M_i}{2|\mathbf{r}-\mathbf{r}_i|}\ , \tag{2.8}$$

where M_i ($i=1,\ldots,N$) are integration constants and $\mathbf{r}_i$ is a Euclidean position vector of ith point in conformally flat three-space. We consider only the case with $M_i\geq 0$ in order to guarantee the positivity of the "gravitational mass."

Since, from the Birkhoff's theorem, the spherically symmetric vacuum space-time with Λ is either the de Sitter or Schwarzschild–de Sitter space-time, the $N=1$ solution is just a three-dimensional spacelike cross section of the Schwarzschild–de Sitter space-time. The gravitational mass M in the Schwarzschild–de Sitter space-time agrees with the present mass parameter M_1 (see Appendix A) [10]. It should be noticed that, by virtue of the condition (2.4), the ordinary asymptotically flat condition corresponds to the asymptotically de Sitter one in our case. In the one-Einstein-Rosen-bridge case, there are two de Sitter-like asymptotic regions: $|\mathbf{r}-\mathbf{r}_1|\to\infty$ and $|\mathbf{r}-\mathbf{r}_1|\to 0$.

The solution with N Einstein-Rosen bridges has a similar asymptotic structure as the Schwarzschild–de Sitter space-time as $|\mathbf{r}-\mathbf{r}_i|\to\infty$. There also exists the Schwarzschild–de Sitter-like asymptotic region

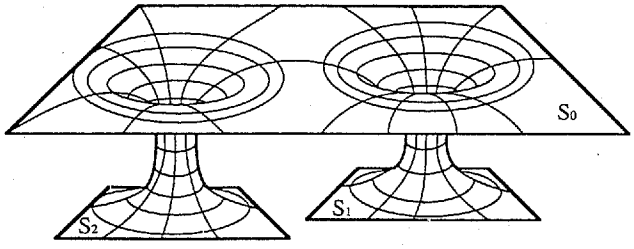

FIG. 1. A two-dimensional embedding of the initial spacelike hypersurface of a space-time containing Einstein-Rosen bridges.

$|\mathbf{r}-\mathbf{r}_i|\to 0$ and therefore there are $(N+1)$-asymptotically Schwarzschild–de Sitter sheets. Hereafter, S_i denotes the ith asymptotic region. S_0 is defined as the three-dimensional sheet including the asymptotic region of $|\mathbf{r}-\mathbf{r}_i|\to\infty$ (see Fig. 1). Because of the asymptotically Schwarzschild–de Sitter region and of our choice of the extrinsic curvature (2.4), the gravitational mass of the Einstein-Rosen bridges can be defined in the same manner as in the asymptotically flat case. The "total mass" $M_{\rm tot}$ of N Einstein-Rosen bridges, which means that for observers in the asymptotic region on S_0, is given by [9]

$$M_{\rm tot}=\sum_{i=1}^{N} M_i \ . \tag{2.9}$$

The gravitational mass m_i of the Einstein-Rosen bridge labeled i, which is that for the asymptotic observer on S_i, is obtained as [9]

$$m_i=M_i\left[1+\sum_{j\neq i}\frac{M_j}{2|\mathbf{r}_i-\mathbf{r}_j|}\right] . \tag{2.10}$$

As in the asymptotically flat case, the total mass is different from the sum of the "mass" of each Einstein-Rosen bridge by the gravitational interaction energy [9]. The "interaction energy" $m_{\rm int}$ is given by

$$m_{\rm int}=M_{\rm tot}-\sum_{i=1}^{N} m_i=-\sum_{i=1}^{N}\sum_{j\neq i}\frac{M_i}{|\mathbf{r}_i-\mathbf{r}_j|} \ . \tag{2.11}$$

The interaction energy is always negative and when the distances $|\mathbf{r}_i-\mathbf{r}_j|$ between all black holes are infinite, the interaction energy vanishes.

III. APPARENT HORIZONS

In order to get some physical insight into the inhomogeneities in the space-time with a cosmological constant from our initial data, we shall search for apparent horizons of an N-Einstein-Rosen-bridge solution. We define three types of apparent horizon: i.e., black-hole, cosmological, and white-hole horizons, as a closed two-surface such that the family of a future-directed outgoing null geodesic orthogonal to the surface does not expand or such that the family of future-directed ingoing null geodesics orthogonal to the surface does not converge. Here, *outgoing* means the direction toward the asymptotic region on S_0, while *ingoing* means the opposite direction since we are interested in the behavior of inhomogeneities seen from our side S_0.

To find the apparent horizons, we calculate the expansion rate of congruence of nearby null geodesics orthogonal to a closed two-surface. Let s^k to be the outward spacelike unit normal vector of the closed two-surface. Then the expansion rates of the outgoing null congruence ρ_+ and of ingoing null congruence ρ_- are given by

$$\rho_\pm=\pm D_i s^i+K_{ij}s^i s^j-K \ , \tag{3.1}$$

respectively. We can obtain the apparent horizons by setting $\rho_+=0$ or $\rho_-=0$. In order to see the physical meaning of these apparent horizons, we first consider the one-Einstein-Rosen-bridge solution and then investigate the two-Einstein-Rosen-bridge solution.

A. One Einstein-Rosen bridge

For one-Einstein-Rosen-bridge solution, without loss of generality we can set $\mathbf{r}_1=0$; then we find the solution as

$$dl^2=\psi^4(r)[dr^2+r^2(d\theta^2+\sin^2\theta\, d\varphi^2)] \ , \tag{3.2}$$

with

$$\psi(r)=1+\frac{M}{2r} \ , \tag{3.3}$$

where we have replaced M_1 with M. As already mentioned, the above solution is just a three-dimensional cross section of the Schwarzschild–de Sitter space-time [10].

The expansions $\rho_\pm$ of outgoing and of ingoing null geodesic congruences orthogonal to a spherical surface centered at $r=0$ are given by

$$\rho_\pm(r)=\pm\frac{2}{\psi^2}\left[\frac{1}{r}+2\frac{\partial_r\psi}{\psi}\right]+2H \ , \tag{3.4}$$

respectively. The apparent horizons are obtained as positive roots of $\rho_\pm(r)=0$ and agree with the event horizons of the Schwarzschild–de Sitter space-time (see Appendix A). There are three types of horizons as will be shown below.

We define a critical mass by $M_{\rm crit}\equiv 1/(\sqrt{27}H)$, which turns to be an important mass scale in the present analysis and also in the inflationary scenario. In the case of $M\leq M_{\rm crit}$, we find the following positive roots. For the equation of ingoing horizon, we obtain

$$\begin{aligned} r_1&=\tfrac{1}{2}[R_C-M+\sqrt{R_C(R_c-2M)}] \ , \\ r_2&=\tfrac{1}{2}[R_B-M+\sqrt{R_B(R_B-2M)}] \ , \end{aligned} \tag{3.5}$$

where R_C and R_B are the circumference radius of the cosmological event horizon and black-hole event horizon, respectively, explicit expressions for which are given in Appendix A. For the equation of outgoing horizon, we have

$$\begin{aligned} r_3&=\frac{1}{2}[R_B-M-\sqrt{R_B(R_B-2M)}] \ , \\ r_4&=\frac{1}{2}[R_C-M-\sqrt{R_C(R_C-2M)}] \ . \end{aligned} \tag{3.6}$$

We can show that the following relation is true:

$$r_4 \le r_3 < r_2 \le r_1 \ . \tag{3.7}$$

The equalities in Eq. (3.7) are realized if and only if $M=M_{\rm crit}$. When $M>M_{\rm crit}$, there is no positive root and then there does not exist any apparent horizon.

As shown in Fig. 2(a), the apparent horizon at $r=r_1$ corresponds to the cosmological event horizon for timelike observers along $R=$const lines on S_0. On the other hand, $r=r_2$ is the black-hole event horizon but is observed as a white-hole horizon for observers on S_0. Hence we call the apparent horizons at $r=r_1$ and at $r=r_2$ the cosmological apparent horizon (CAH) and the white-hole apparent horizon (WAH), respectively. The apparent horizon at $r=r_3$ also corresponds to the black-hole event horizon but is observed just as a black-hole horizon for timelike observers on S_0 and hence we call it the black-hole apparent horizon (BAH). The apparent horizon at $r=r_4$ corresponds to the cosmological event horizon for timelike observers along $R=$const lines on S_1 and has nothing to do with observers on S_0.

B. Two Einstein-Rosen bridges

For simplicity, we consider cases in which each Einstein-Rosen bridge has an equal mass, i.e., $M_1=M_2=M$. The conformal factor ψ of the two-Einstein-Rosen-bridge solution is written as

$$\psi=1+\frac{M}{2\sqrt{r^2+r_0^2-2r_0r\cos\theta}}+\frac{M}{2\sqrt{r^2+r_0^2+2r_0r\cos\theta}}\ , \tag{3.8}$$

where r_0 is half of the Euclidean distance between two Einstein-Rosen bridges. Here (r,θ) is the spherical coordinates in the conformally flat three-space whose origin is chosen to be the center of two Einstein-Rosen bridges. The gravitational mass m of each Einstein-Rosen bridge is given by

$$m=M\left[1+\frac{M}{4r_0}\right] . \tag{3.9}$$

If r_0 is enough larger, i.e., $r_0 \gg M$, each Einstein-Rosen bridge can be seen as an isolated system with mass M. Hence, in such a circumstance, each Einstein-Rosen bridge has the same kind of apparent horizons as the one Einstein-Rosen bridge. On the other hand, if r_0 is not so large and the interaction energy $m_{\rm int}$ is not negligible, each Einstein-Rosen bridge cannot be seen as an isolated system. We expect that there is some influence for the apparent horizons by the interaction between those Einstein-Rosen bridges. In fact, for the $\Lambda=0$ case, as r_0 decreases, the black-hole apparent horizon surrounding both Einstein-Rosen bridges appears. Thus one may expect that one black hole is formed by observers on S_0, if two Einstein-Rosen bridges are sufficiently close. We shall, hence, investigate the apparent horizons formed near those Einstein-Rosen bridges. In order to obtain the BAH, WAH and CAH, we adopt the prescription proposed by Sasaki *et al.* (see Appendix B) [11]. Here it should be noticed that since the interaction energy $m_{\rm int}$ is a monotonically decreasing function of r_0, we can recognize r_0 as a measure of the distance between two bridges. Furthermore, as seen in Fig. 3, the proper distance r_p be-

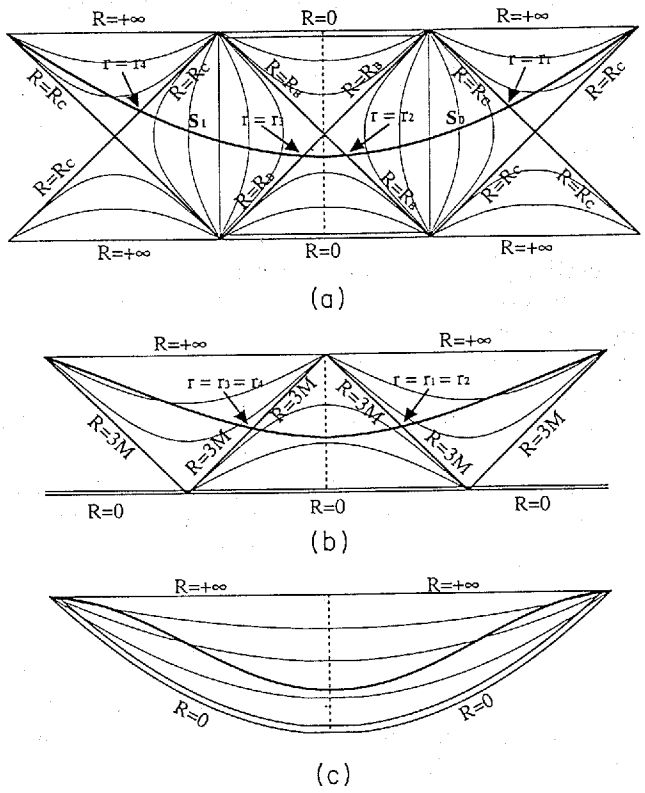

FIG. 2. The Penrose diagrams of the Schwarzschild–de Sitter space-time. (a), (b), and (c) correspond to those with $M<M_{\rm crit}$, $M=M_{\rm crit}$, and $M>M_{\rm crit}$, respectively. The spacelike hypersurface given in Sec. III is depicted by the thick solid line in each Penrose diagram. The dashed line and thin solid curves correspond to the position of the minimal surface and $R=$const curves, respectively.

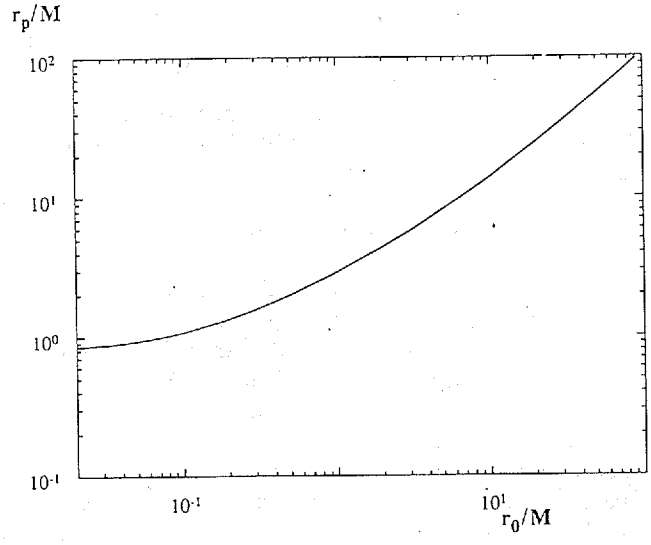

FIG. 3. The proper distance r_p between the minimal surfaces of each bridge is plotted with respect to r_0. R_p is the monotonically increasing function of r_0. Hence, we can regard r_0 as a measure of the separation between two bridges.

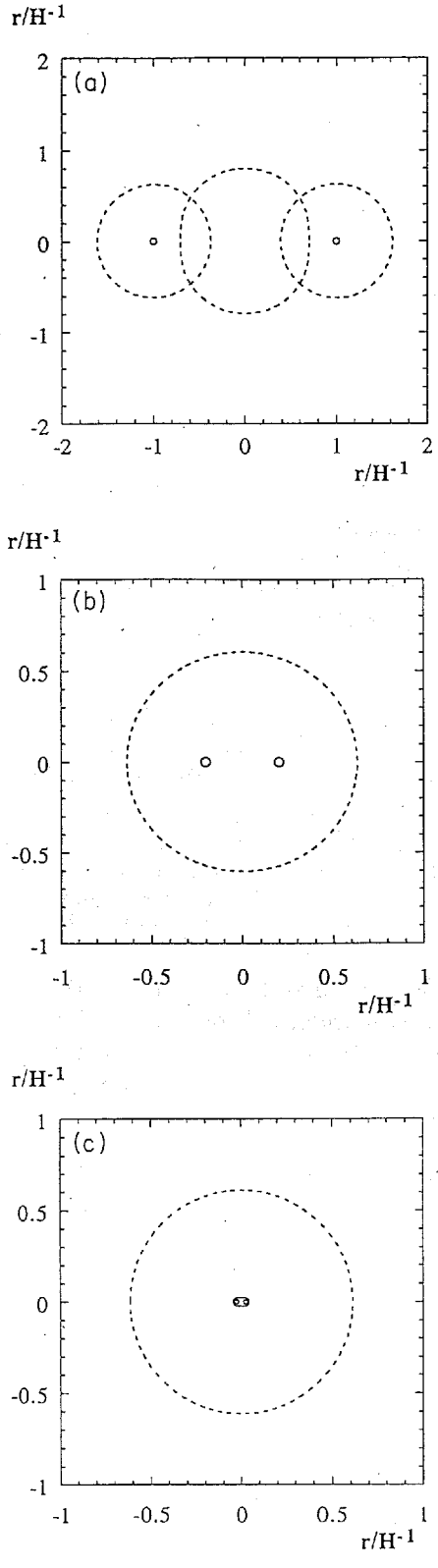

FIG. 4. BAH's and CAH's are depicted in the conformally flat three-space for (a) $M=0.7M_{\rm crit}$, $r_0=\mathrm{H}^{-1}$, (b) $M=0.4M_{\rm crit}$, $r_0=0.2\ \mathrm{H}^{-1}$, and (c) $M=0.4M_{\rm crit}$, $r_0=0.05\ \mathrm{H}^{-1}$. The solid circles are BAH's enclosing each bridge, while the dashed circles correspond to CAH's. In case (a), each bridge can be seen as an isolated system, while in cases (b) and (c), each bridge cannot be regarded as an isolated system. In particular, for case (c), the BAH enclosing two bridges appears and two bridges will collapse into one black hole.

tween the minimal surfaces of two bridges monotonically increases with respect to r_0. Hence, in the following discussion, we adopt r_0 as the measure of the distance between two bridges.

In order to get a qualitative understanding, we show examples of BAH's and CAH's in Fig. 4. The solid circles are the BAH while the dashed circles correspond to the CAH. In Fig. 4(a), the gravitational mass M is equal to $0.7M_{\rm crit}$ and the separation r_0 is H^{-1}. In this case, each bridge can be seen as an isolated system. Figure 4(b) is the same as Fig. 4(a) but with $M=0.4M_{\rm crit}$ and with $r_0=0.2\ \mathrm{H}^{-1}$. There exists a CAH which encloses two bridges and hence we cannot regard each bridge as an isolated system. Figure 4(c) is also the same as Fig. 4(a) but with $M=0.4M_{\rm criit}$ and with $r_0=0.05\ \mathrm{H}^{-1}$. In this case, a BAH appears surrounding two bridges and forms one black hole. We shall discuss more quantitative analysis below.

1. *Black-hole apparent horizons*

We present numerical examples for $M=0.1M_{\rm crit}$, $0.7M_{\rm crit}$, and $2.0M_{\rm crit}$ and discuss first about whether or not a BAH exists as changing the distance r_0 of two bridges.

In the case of $M=0.1M_{\rm crit}$, since the total mass $M_{\rm tot}$ of this system is smaller than $M_{\rm crit}$ and since this system agrees with the one-Einstein-Rosen-bridge case with $2M(<M_{\rm crit})$ as $r_0\to 0$, we expect that a BAH appears surrounding two Einstein-Rosen bridges when those bridges are close enough to each other. In the case of the asymptotically flat space-time without Λ, BAH's appear inside black-hole event horizons [12]. Hence, when the BAH surrounding two Einstein-Rosen bridges appears, those bridges are also surrounded by a black-hole event horizon. Of course, in general, it might not be true in the case with a nonvanishing Λ. However, we can prove that BAH's in our initial data also appear inside the black-hole event horizon, which is defined by the boundary of the causal past of the future conformal infinity, as in the asymptotically flat space-time without Λ [13]. Hence, also in the present case, the existence of the BAH surrounding two Einstein-Rosen bridges means that these two bridges collide with each other and form one black hole. In Fig. 5, for $M=0.1M_{\rm crit}$, we show the proper area of the BAH enclosing just one Einstein-Rosen bridge by the dashed line and twice that by the dot-dashed line, which means the total area of the BAH's surrounding each bridge, with respect to r_0. The solid line denotes the BAH enclosing both bridges. As r_0 decreases, the proper area of the BAH enclosing each bridge increases since the gravitational mass m of each Einstein-Rosen bridge increases with respect to r_0 for fixed $M_{\rm tot}$. The proper area of the BAH enclosing two bridges is almost constant with respect to r_0 but does not appear for $r_0>1.20\times10^{-2}$ H^{-1}, where the total area of BAH's by each bridge becomes equal to the proper area of BAH by two bridges.

When $M=0.7M_{\rm crit}$, i.e., $M_{\rm tot}=1.4M_{\rm crit}$, as expected, BAH, which surrounds two Einstein-Rosen bridges, does not appear, while the BAH enclosing each bridge exists. The proper area of the BAH enclosing each bridge is

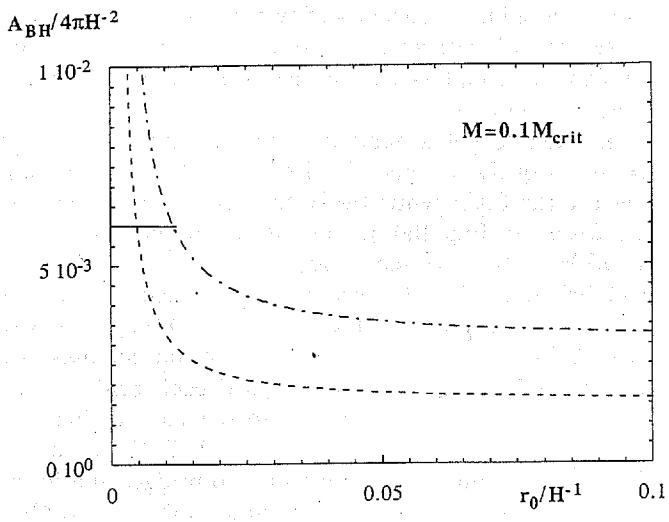

FIG. 5. The proper area of the BAH for $M=0.1M_{crit}$ is plotted with respect to r_0/H^{-1}. The solid line denotes the area of the BAH enclosing two Einstein-Rosen bridges, while the dashed line corresponds to that enclosing each bridge.

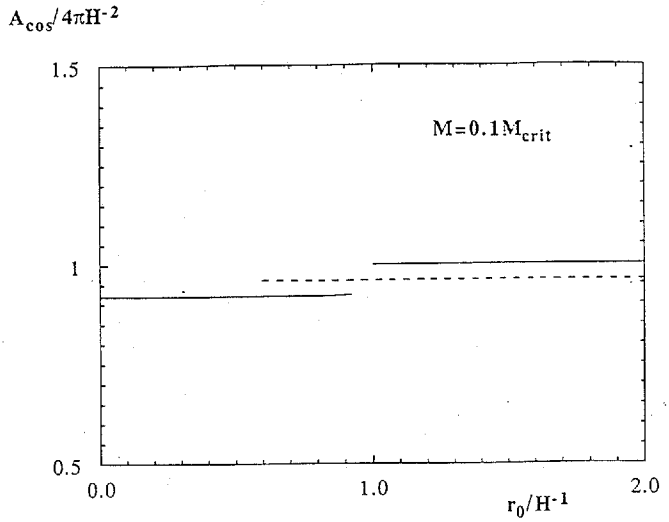

FIG. 7. The proper area of the CAH for $M=0.1M_{crit}$ is plotted with respect to r_0/H^{-1}. The solid line denotes that of the CAH centered at the origin, while the dashed line shows that of CAH enclosing each bridge.

plotted with respect to r_0 in Fig. 6. For the same reason as in the case of $M=0.1M_{crit}$, the proper area increases as r_0 decreases. It is worth noticing that the BAH enclosing each bridge vanishes for $r_0<7.86\times10^{-2}\ H^{-1}$ or equivalently for $m>1.00M_{crit}$. In the case of $M=2.0M_{crit}$, no BAH appears.

2. *Cosmological apparent horizons*

The CAH gives us some physical insight about the cosmic expansion effect by Λ. Here it should be noticed that since our initial data becomes a de Sitter universe in the asymptotically far region from those Einstein-Rosen bridges, $\rho_-=0$ has no unique solution for a CAH. We have to specify a point in the space-time which is enclosed by one CAH. Since we are interested in the effect of the Einstein-Rosen bridges on cosmic expansion, we investigate the existence of a CAH which is centered at the origin, and that which encloses just one Einstein-Rosen bridge, for the same initial data as the cases of the BAH. In Fig. 7, the proper area of a CAH for the case of $M=0.1M_{crit}$ is plotted with respect to r_0 by the solid line for that centered at the origin, and by the dashed line for that enclosing each bridge. Figures 8 and 9 are the same as Fig. 7 but with $M=0.7M_{crit}$ and $2.0M_{crit}$, respectively.

In the case of $M=0.1M_{crit}$, the CAH enclosing each Einstein-Rosen bridge cannot be found for $r_0<0.60\ H^{-1}$. It may move to the CAH enclosing both bridges and change its proper area just as happens for the CAH centered at the origin as we will show below. For $r_0>0.60\ H^{-1}$, the proper area of a CAH enclosing each bridge is almost constant and the same as that of the one-Einstein-Rosen-bridge case with the gravitational mass

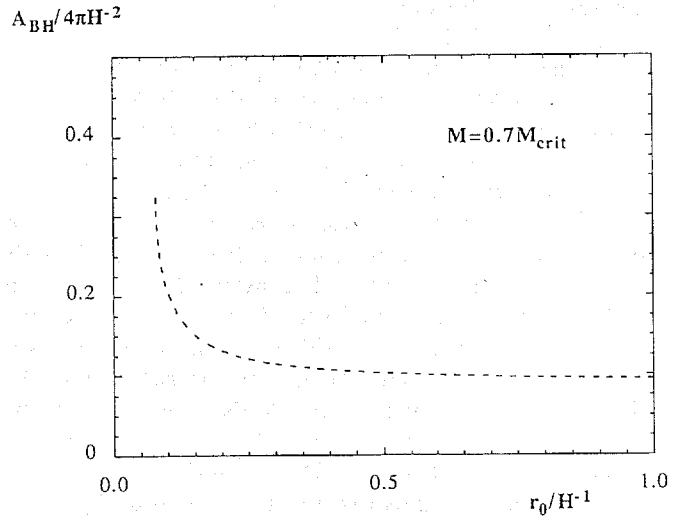

FIG. 6. Same as Fig. 3 but for $M=0.7M_{crit}$. In this case, there is no BAH enclosing two bridges.

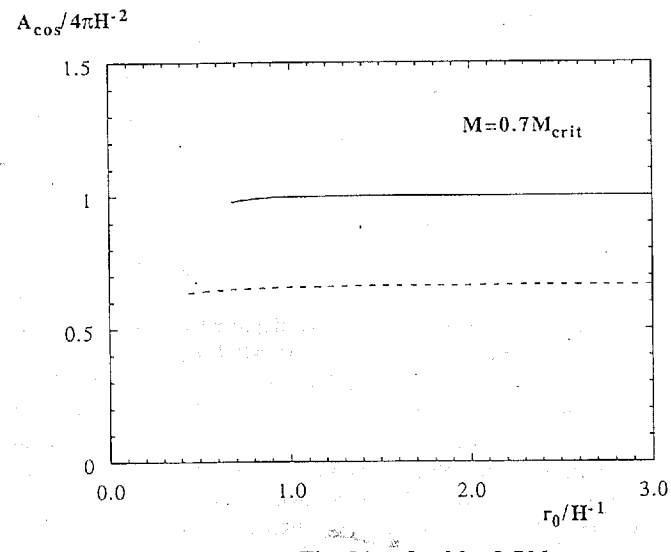

FIG. 8. Same as Fig. 5 but for $M=0.7M_{crit}$.

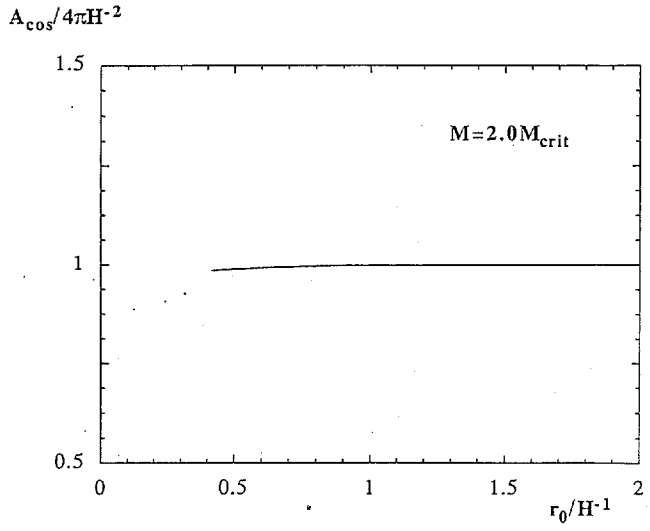

FIG. 9. Same as Fig. 5 but for $M=2.0M_{crit}$. In this case, there is no CAH enclosing each bridge.

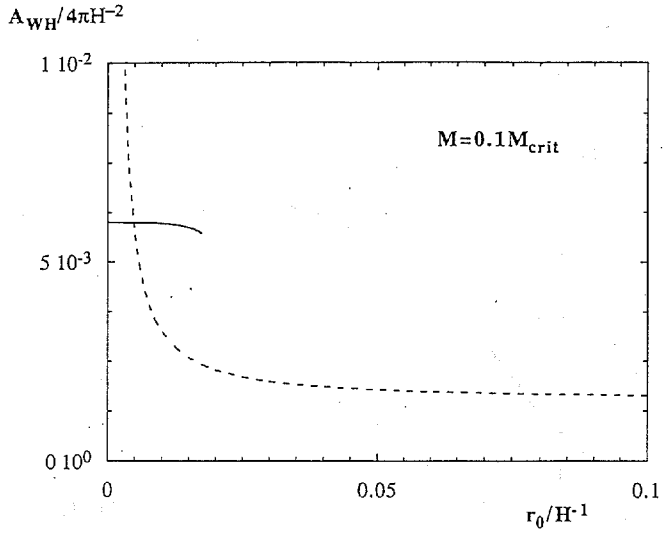

FIG. 10. The proper area of the WAH for $M=0.1M_{crit}$ is plotted with respect to r_0/H^{-1}. The solid line denotes that of the WAH enclosing two bridges, while the dashed line corresponds to that of the WAH enclosing each bridge.

$M=0.1M_{crit}$, i.e., $0.96\times 4\pi\ H^{-2}$. On the other hand, the proper area of a CAH centered at the origin is equal to that of de Sitter space-time, $4\pi\ H^{-2}$, for $r_0 > H^{-1}$, while, for $r_0 < 0.92\ H^{-1}$, the proper area of the CAH is almost the same as that of the Schwarzschild–de Sitter space-time with the gravitational mass $M=0.2M_{crit}$, which is $0.92\times 4\pi\ H^{-2}$. This reason is simple because the CAH for $r_0 > H^{-1}$ exists between two bridges while that for $r_0 < 0.92\ H^{-1}$ encloses two bridges. For $0.92\ H^{-1} < r_0 < H^{-1}$, we could not find the CAH centered at the origin numerically. We may understand this difficulty because the regions enclosed by the CAH for $r_0 < 0.92\ H^{-1}$ are topologically different from that for $r_0 > H^{-1}$.

In the case of $M=0.7M_{crit}$, the proper area of the CAH centered at the origin is constant and equal to that of de Sitter space-time as long as $r_0 \gtrsim H^{-1}$. However, as expected from the one bridge case, once $r_0 < 0.68\ H^{-1}$, the CAH centered at the origin disappears. The CAH surrounding each bridge also vanishes for $r_0 < 0.44\ H^{-1}$ or equivalently for $m > 0.737M_{crit}$. In the case of $M=2.0M_{crit}$, the CAH enclosing each Einstein-Rosen bridge does not exist, while that centered at the origin appears as long as $r_0 > 0.42\ H^{-1}$.

Here it should be noted that when $r_0 > H^{-1}$, the proper area of the BAH and CAH enclosing each bridge almost agrees with those of the one-Einstein-Rosen-bridge case. Furthermore, with this separation, the proper area of the CAH centered at the origin is almost the same as that of de Sitter space-time. Hence, each Einstein-Rosen bridge is regarded as an isolated system if $r_0 > H^{-1}$.

3. *White-hole apparent horizon*

For completeness, we also analyze a WAH. We show the proper area of the WAH for the cases with $M=0.1M_{crit}$ and of $M=0.7M_{crit}$ in Figs. 10 and 11, respectively, with respect to r_0. In the case of $M=2.0M_{crit}$, there is no WAH. In Fig. 10, the dashed line denotes the proper area of the WAH enclosing each bridge and the solid line corresponds to that of the WAH enclosing two bridges.

The WAH enclosing each bridge is the BAH for asymptotic observers in S_1 and S_2. In the case of $M=0.7M_{crit}$, the WAH enclosing each bridge vanishes at $r_0 \simeq 8.3\times 10^{-2}\ H^{-1}$, when the proper area is about $0.29\times 4\pi\ H^{-2}$. The gravitational mass for the asymptotic observers in S_1 or in S_2 is $m \simeq 0.98M_{crit}$ for $r_0 \simeq 8.3\times 10^{-2} H^{-1}$. In the case of $M=0.1M_{crit}$, we also expect that the WAH enclosing each bridge disappears for $m=M_{crit}$, i.e., $r_0 \simeq 1.07\times 10^{-3}\ H^{-1}$, but we could not confirm it numerically because of such a small separation.

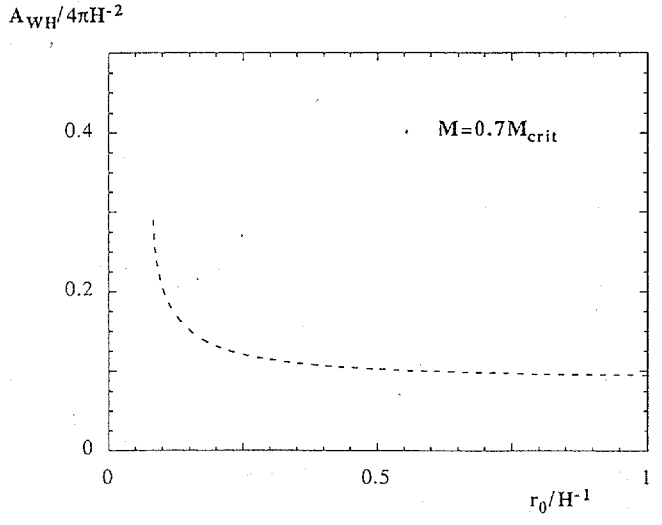

FIG. 11. Same as Fig. 9 but for $M=0.7M_{crit}$. As in the case of BAH, there is no WAH enclosing two bridges.

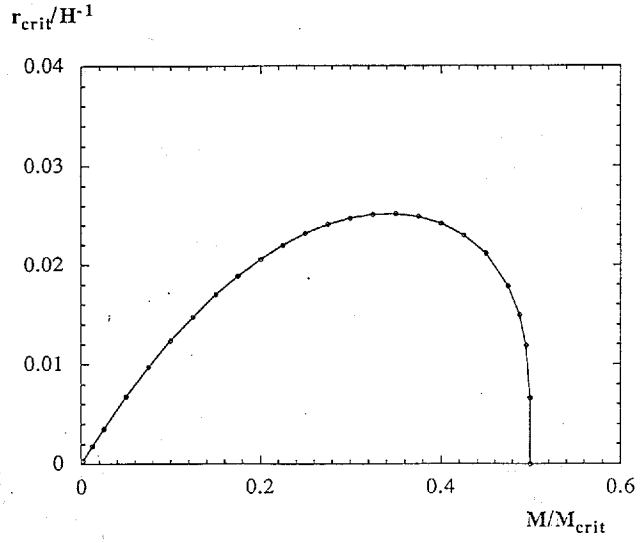

FIG. 12. We show the relation between the critical separation r_{crit}, at which the BAH enclosing two bridges appears first, and the gravitational mass M. For $M > 0.35M_{crit}$, r_{crit} decreases as M increases. The maximum value of r_{crit} turns out to be $\sim 0.025\ H^{-1}$.

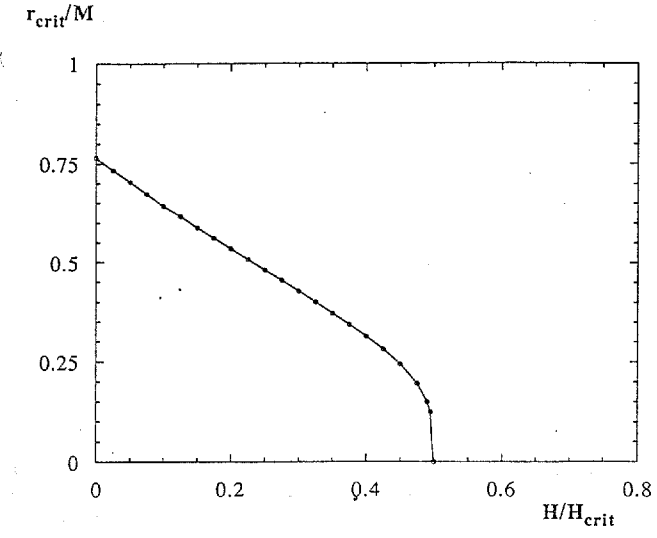

FIG. 14. For fixed M, we show the relation between r_{crit} and H/H_{crit}, where $H_{crit} \equiv 1/(\sqrt{27}M)$. The critical separation monotonically decreases with respect to H/H_{crit}.

Critical separation

We shall estimate numerically the critical separation r_{crit} such that the BAH surrounding two Einstein-Rosen bridges disappears for $r_0 > r_{crit}$. In Fig. 12, we show r_{crit}/H^{-1} with respect to the gravitational mass M/M_{crit}. In the case of the asymptotically flat space without Λ, $r_{crit} = 0.766M$ [14]. This means that the large gravitational mass produces strong gravity, by which the BAH enclosing two massive bridges appears even for a large distance. On the other hand, in our case with nonvanishing Λ, r_{crit} does not monotonically increase with respect to M but has a maximum value at $M \sim 0.35M_{crit}$. Hence, it seems that the Einstein-Rosen bridges with a large gravitational mass are hard to coalesce with each other to form a black hole if Λ exists. In Fig. 13, the proper area of a BAH surrounding two Einstein-Rosen bridges with $r_0 = r_{crit}$ is plotted with respect to M/M_{crit}, as shown by the solid line. The dashed line corresponds to that with $r_0 = 0$, i.e., that of the one-Einstein-Rosen-bridge case with $M_{tot} = 2M$. It should be noted that the proper area of the BAH with $r_0 = r_{crit}$ is always larger than that of the one-Einstein-Rosen-bridge case with the same M_{tot}.

In Fig. 14, r_{crit}/M is also plotted with respect to H/H_{crit} for fixed M, where $H_{crit} \equiv 1/(\sqrt{27}M)$. As expected, the critical separation r_{crit} monotonically decreases with respect to H/H_{crit}. The cosmic expansion

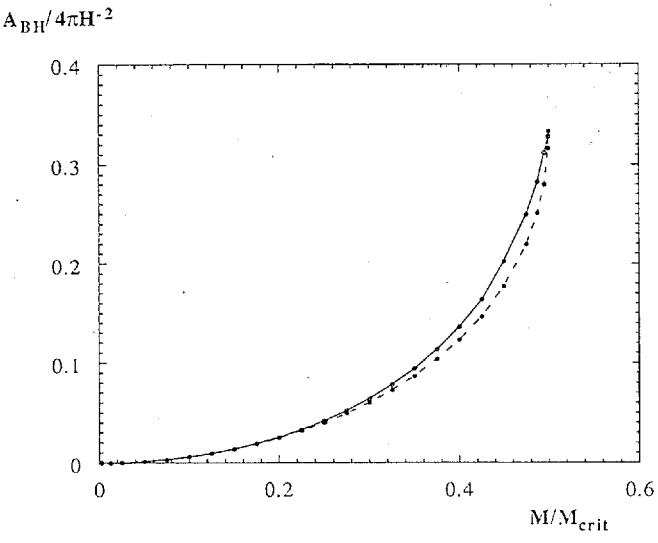

FIG. 13. The proper area of the BAH enclosing two bridges with $r_0 = r_{crit}$ is plotted with respect to M by the solid line. The dashed line denotes the proper area of the one-Einstein-Rosen-bridge case.

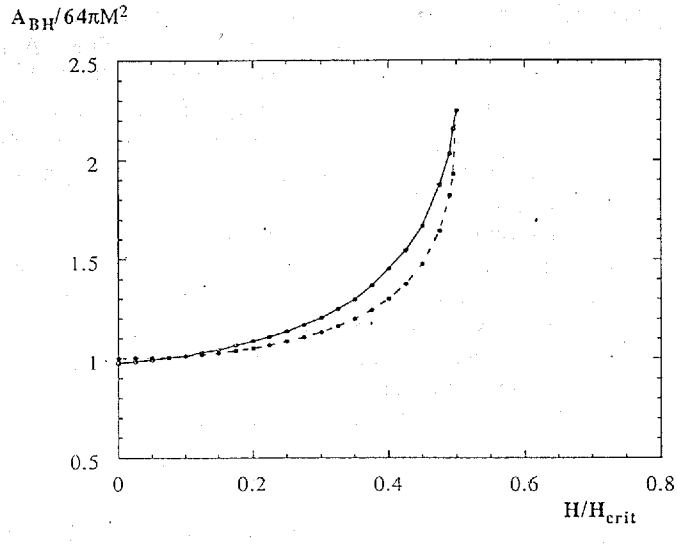

FIG. 15. The proper area of the BAH enclosing two bridges with $r_0 = r_{crit}$ is plotted with respect to H/H_{crit} by the solid line. The dashed line denotes the proper area of the one-Einstein-Rosen-bridge case.

due to Λ seems to prevent two bridges from coalescing with each other and forming one larger black hole. In Fig. 15, the proper area of a BAH surrounding two bridges is plotted with respect to $H/H_{\rm crit}$ with $r_0=r_{\rm crit}$, while the dashed line denotes that of $r_0=0$, i.e., that of the one-bridge case. In this case with large Λ, the proper area of a BAH with $r_0=r_{\rm crit}$ is also larger than that of the one-bridge case with the same $M_{\rm tot}$, although it becomes the opposite for small Λ just as in the $\Lambda=0$ case.

IV. SUMMARY AND DISCUSSION

We have presented N-Einstein-Rosen-bridge solutions in the space-time with a cosmological constant and analyzed three types of apparent horizons for one- and two-Einstein-Rosen-bridge cases. The one-Einstein-Rosen-bridge solution corresponds to a spacelike cross section of the Schwarzschild–de Sitter space-time and brings us important insight into the features of our present problem. The global structure of this space-time depends on M. When $M<M_{\rm crit}$, there is a black hole with a cosmological event horizon. On the other hand, if $M\geq M_{\rm crit}$, this space-time does not have a black hole but does approach de Sitter space-time asymptotically locally assuming that the space-time is initially expanding. Correspondingly a BAH and a CAH exist in the case of $M<M_{\rm crit}$, while both the BAH and CAH disappear in the case of $M>M_{\rm crit}$. When $M=M_{\rm crit}$, the BAH and the CAH coincide with each other.

In the case of two Einstein-Rosen bridges, the existence of the BAH or the CAH essentially follows the same criterion of one-Einstein-Rosen-bridge case. The BAH enclosing two Einstein-Rosen bridges does not exist when the total mass $M_{\rm tot}$ is larger than $M_{\rm crit}$ even if the distance between two bridges is very short. In fact, the critical separation $r_{\rm crit}$, such that the BAH surrounding two bridges disappears for the separation $r_0>r_{\rm crit}$, has a maximum value $r_0\sim 0.025\ {\rm H}^{-1}$ at $M\sim 0.35M_{\rm crit}$, beyond which $r_{\rm crit}$ decreases. Furthermore, the CAH enclosing two bridges also disappears in this case. Hence, unless a part of the total mass is released in some way (e.g., by gravitational radiation), it seems impossible for two Einstein-Rosen bridges with a large mass to coalesce with each other and form one black hole.

Although, in this paper, we have analyzed the apparent horizons under the condition of a uniformly expanding background, we can also find the analytic solution for N Einstein-Rosen bridges with a cosmological constant under the condition of a uniformly collapsing background; i.e., imposing the condition for the initial hypersurface,

$$K_i^j=H\delta_i^j\ , \tag{4.1}$$

we can obtain the same intrinsic metric as Eq. (2.8), but the direction of time evolution is downward in Fig. 2. Hence, all of space-time collapses into a singularity in the case of $M\geq M_{\rm crit}$, while for $M<M_{\rm crit}$, a black-hole singularity appears as in the uniformly expanding background case. Although we can discuss the apparent horizons in this case, it may not be so interesting from the point of view of the cosmic no hair conjecture.

The examples we have shown here are just initial data; however, from the analysis of these data, we may get some physical insight about the dynamics of inhomogeneous space-time with a cosmological constant. One of the most important conjectures, which we find from the present analysis, is that there is an upper bound on the areas of apparent horizons in space-time with a cosmological constant: i.e.,

$$A\leq 4\pi\,{\rm H}^{-2}\ . \tag{4.2}$$

In fact, we can prove that the inequality (4.2) is true for initial data with $K_i^j=\frac{1}{3}K\delta_i^j$, where K is a constant [13]. We can also conjecture that the area of event horizons in a stationary space-time also has the same bound. This is true for a static space-time with a single cosmological horizon [15]. We can also prove the black-hole area theorem in de Sitter background [13]. The area of the black-hole event horizons must increase in time just as in the case of asymptotically flat space-time. Suppose that the Universe approaches a stationary space-time. There is, then, likely to exist an upper bound also on the black-hole event horizon in de Sitter background, i.e., $A_{\rm BH}\leq 4\pi\ {\rm H}^{-2}$. This fact with the above area theorem, hence, yields the following expectation: Black holes in de Sitter background cannot coalesce with each other beyond the critical area of the event horizon, resulting that many small black holes still remain in de Sitter background.

This expectation brings us to a desirable inflationary scenario in inhomogeneous space-times as follows. Initial inhomogeneities collapse into many small black holes, the areas of which are bounded as $A_{\rm BH}\leq 4\pi\ {\rm H}^{-2}$, but not into large-scale inhomogeneities which may prevent the global portion of the Universe expanding exponentially, if the cosmic censorship hypothesis is true. These small black holes are harmless in an inflationary scenario, because they will not only be diluted away by the exponential expansion of the Universe but will also be evaporated away soon by Hawking radiation. [The typical mass of the black holes is $\sim 10^2$ g for grand unified theory-scale vacuum energy.] In order to confirm this scenario, the research concerning the above discussion is now in progress.

ACKNOWLEDGMENTS

We would like to thank our colleagues in the Departments of Physics in Kyoto University and in Waseda University for their helpful discussion. K.N. is grateful to H. Sato and M. Sasaki for their stimulating discussion. K.Y. also wishes to thank Y. Yamanaka and J. Yokoyama for their useful discussion. This work was partially supported by the Grant-in-Aid for Scientific Research of the Ministry of Education No. 1526, No. 04234211, and No. 04640312.

APPENDIX A

By the use of the Schwarzschild coordinates, the metric of the Schwarzschild-de Sitter space-time is written as

$$ds^2=-CdT^2+C^{-1}dR^2+R^2(d\theta^2+\sin^2\theta\, d\varphi^2)\ , \tag{A1}$$

with

$$C=1-\frac{2M}{R}-H^2R^2\ , \tag{A2}$$

where M is the gravitational mass.

As the Schwarzschild space-time, $C=0$ gives the positions of event horizons. However, there does not exist a positive root of $C=0$ if $M>M_{\rm crit}\equiv 1/(\sqrt{27}\ {\rm H})$. On the other hand, in the case of $M\le M_{\rm crit}$, we obtain the following positive roots:

$$R_B=\frac{2}{H\sqrt{3}}\cos[\tfrac{1}{3}(\pi+\arctan\sqrt{\omega_e})]\ ,$$
$$R_C=\frac{2}{H\sqrt{3}}\cos[\tfrac{1}{3}(\pi-\arctan\sqrt{\omega_e})]\ , \tag{A3}$$

where

$$\omega_e\equiv\frac{1}{27M^2H^2}-1\ . \tag{A4}$$

It is always true that $R_B\le R_C$. $R_B=R_C(=3M)$ is realized if $M=M_{\rm crit}$. The Penrose diagrams for $M<M_{\rm crit}$, $M=M_{\rm crit}$, and $M>M_{\rm crit}$ are depicted in Figs. 2(a), 2(b), and 2(c), respectively. In the case of $M<M_{\rm crit}$, R_B is regarded as the position of the black-hole event horizon, while R_C is the position of cosmological event horizon for timelike observers along $R=$const lines.

In the case of $M<M_{\rm crit}$, there is the static timelike Killing vector and hence the Penrose diagram has a reflection symmetry with respect to the timelike direction. On the other hand, since there is no static timelike Killing vector in the case of $M>M_{\rm crit}$, we should introduce a direction of the time evolution, in order to discuss the causal structure. Our initial hypersurface (3.2) is embedded in the Schwarzschild–de Sitter space-time as depicted by the thick solid line in Fig. 2 and the direction of its time evolution is upward in this figure due to the condition of the uniformly expanding background universe (2.4) [16]. Along this direction, the black-hole singularity is formed for $M<M_{\rm crit}$, while the space-time approaches the de Sitter space-time asymptotically and a black-hole singularity does not appear in the case of $M\ge M_{\rm crit}$. Hence, in the case of $M\ge M_{\rm crit}$, there is no black-hole event horizon. However, it should be noted that there is always an event horizon for any observer along a timelike curve λ, which is defined by the boundary of the causal past of λ, i.e., $J^-(\lambda)$ [17], but, in general, this does not agree with the apparent horizon, in particular, for a dynamical problem.

APPENDIX B

We assume the topology of the apparent horizon is S^2. As long as the deviation of the shape of the apparent horizon from a sphere is not so large, this surface is expressed as

$$r=r(\theta)\ , \tag{B1}$$

where $r=r(\theta)$ is assumed to be a single-valued function. Then the equation for the apparent horizon $\rho_\pm=0$ is written as

$$\frac{d^2r}{d\theta^2}=A_3\left[\frac{dr}{d\theta}\right]^3+A_2\left[\frac{dr}{d\theta}\right]^2+A_1\left[\frac{dr}{d\theta}\right]+{}^{(\pm)}A_0\ , \tag{B2}$$

where

$${}^{(\pm)}A_0=2r(1+2r\psi^{-1}\partial_r\psi)\mp 2HN\ , \tag{B3}$$
$$A_1=-\cot\theta-4\psi^{-1}\partial_\theta\psi\ , \tag{B4}$$
$$A_2=r^{-1}(3+4r\psi^{-1}\partial_r\psi)\ , \tag{B5}$$
$$A_3=-r^{-2}(\cot\theta+4\psi^{-1}\partial_\theta\psi)\ , \tag{B6}$$

with

$$N=r\psi^{-1}\left[r^2+\left[\frac{dr}{d\theta}\right]^2\right]^{-3/2}\ . \tag{B7}$$

Here ${}^{(+)}A_0$ is taken for $\rho_+=0$ and ${}^{(-)}A_0$ for $\rho_-=0$. Since our system is axisymmetric, the boundary condition is imposed on the symmetric axis as

$$\frac{dr}{d\theta}=0\ \text{ at }\theta=0\text{ and }\pi\ . \tag{B8}$$

We solve the above equation iteratively by the use of the finite difference method. However, there is no solution or no unique solution under the above boundary condition. As pointed by Sasaki *et al.*, in order to overcome this difficulty, we add a certain term to both sides of Eq. (B2):

$$\frac{d^2r}{d\theta^2}+w_0r=A_3\left[\frac{dr}{d\theta}\right]^3+A_2\left[\frac{dr}{d\theta}\right]^2+A_1\left[\frac{dr}{d\theta}\right]+A_0+w_0r\ , \tag{B9}$$

where w_0 is a constant.

For the case of one Einstein-Rosen bridge, there are two positive roots r_1 and r_2 for $\rho_-=0$ and there are also two positive roots r_3 and R_4 for $\rho_+=0$. Hence, if we solve Eq. (B9) by the iteration method with fixed w_0, we can obtain one of two roots for $\rho_-=0$ or for $\rho_+=0$. Consequently, if we take $w_0>0$, we can obtain r_1 and r_4, while we choose $w_0<0$ in order to get r_2 and r_3. In the case of two Einstein-Rosen bridges, we can obtain the apparent horizons corresponding to those for one-Einstein-Rosen-bridge case by the appropriate choice of w_0.

[1] A. H. Guth, Phys. Rev. D **23**, 347 (1981); K. Sato, Mon. Not. R. Astron. Soc. **195**, 467 (1981); A. Albrecht and P. J. Steinhardt, Phys. Rev. Lett. **48**, 1220 (1982); A. D. Linde, Phys. Lett. **108B**, 389 (1982).

[2] G. W. Gibbons and S. W. Hawking, Phys. Rev. D **15**, 2738 (1977); S. W. Hawking and I. G. Moss, Phys. Lett. **110B**, 35 (1982); as for a review, see also, e.g., K. Maeda, in *Fifth Marcel Grossmann Meeting,* Proceedings, Perth, Australia, 1988, edited by D. G. Blair and M. J. Buckingham (World Scientific, Singapore, 1989), p. 145.

[3] K. Sato, M. Sasaki, H. Kodama, and K. Maeda, Prog. Theor. Phys. **65**, 1443 (1981); K. Maeda, K. Sato, M. Sasaki, and H. Kodama, Phys. Lett. **108B**, 98 (1982); K. Sato, in The Large Scale Structure of the Universe, Proceedings of IAU Symposium No. 130 (unpublished).

[4] E. Calzetta and M. Sakellariadou, Phys. Rev. D **45**, 2802 (1992).

[5] H. Kurki-Suonio, J. Centrella, R. A. Matzner, and J. R. Wilson, Phys. Rev. D **35**, 435 (1987); P. Laguna, H. Kurki-Suonio, and R. A. Matzner, *ibid.* **44**, 3077 (1991); K. A. Holcomb, S. J. Park, and E. T. Vishniac, *ibid.* **39**, 1058 (1989); D. S. Goldwirth and T. Piran, *ibid.* **40**, 3263 (1989); Phys. Rev. Lett. **64**, 2852 (1990).

[6] D. Garfinkle and C. Vuille, Gen. Relativ. Gravit. **23**, 471 (1991).

[7] K. Nakao, Gen. Relativ. Gravit. **24**, 1069 (1992).

[8] K. Nakao, K. Maeda, T. Nakamura, and K. Oohara, preceding paper, Phys. Rev. D **47**, 3194 (1993).

[9] D. R. Brill and R. W. Lindquist, Phys. Rev. **131**, 471 (1963).

[10] B. Carter, Commun. Math. Phys. **17**, 1067 (1970); in *Black Holes,* edited by C. DeWitt and B. S. DeWitt (Gordon and Breach, New York, 1972); G. W. Gibbons and S. W. Hawking, in The Large Scale Structure of the Universe Proceedings of the I.A.U. Symposium No. 130 (unpublished) [3].

[11] M. Sasaki, K. Maeda, S. Miyama, and T. Nakamura, Prog. Theor. Phys. **63**, 1051 (1980).

[12] S. W. Hawking, in *Black Holes* [10].

[13] T. Shiromizu, K. Nakao, H. Kodama, and K. Maeda (unpublished).

[14] A. Cadez, Ann. Phys. (N.Y.) **43**, 449 (1974).

[15] W. Boucher and G. W. Gibbons, Phys. Rev. D **30**, 2447 (1984).

[16] K. Nakao, K. Maeda, T. Nakamura, and K. Oohara, Phys. Rev. D **44**, 1326 (1991).

[17] Gibbons and Hawking in [2].